Quantum and Classical Coincidence Imaging

Ryan S. Bennink,* Sean J. Bentley,[†] and Robert W. Boyd

The Institute of Optics, University of Rochester, Rochester, New York 14627, USA

John C. Howell

Department of Physics and Astronomy, University of Rochester, Rochester, New York 14627, USA

Coincidence, or ghost, imaging is a technique that uses two correlated optical fields to form an image of an object. In this work we identify aspects of coincidence imaging which can be performed with classically correlated light sources and aspects which require quantum entanglement. We find that entangled photons allow high-contrast, high-resolution imaging to be performed at any distance from the light source. We demonstrate this fact by forming ghost images in the near and far fields of an entangled photon source, noting that the product of the resolutions of these images is a factor of 3 better than that which is allowed by classical diffraction theory.

The novel properties of quantum entangled light sources have been the subject of many theoretical and experimental studies and have inspired a number of new techniques including intrinsically secure communication [1], quantum teleportation [2], dense coding [3], referenceless measurement calibration [4,5], subwavelength lithography [6–8], and coincidence imaging [9]. Coincidence or "ghost" imaging is a novel imaging method in which the object and imaging system are on different optical paths and are illuminated separately by correlated optical fields. Recently, several of us demonstrated coincidence imaging with the use of two classically correlated beams [10], reproducing some behavior that had previously been demonstrated only with the use of entangled light sources. This result has raised the question of what aspects of coincidence imaging, if any, are distinctly nonclassical, and has prompted some recent discussion [11,12].

In this Letter we distinguish between classical and nonclassical aspects of coincidence imaging. In particular, we demonstrate that coincidence images formed with a fixed geometry, including ghost diffraction patterns, do not reveal any distinctly nonclassical behavior. However, the ability to form images with high resolution and high contrast in any plane, without changing the illumination, *is* a nonclassical signature [11,13]. This signature can be expressed as a violation of an inequality, akin to a Bell inequality [14], which we derive below. In the context of classical wave mechanics, this inequality is manifest in the principle of diffraction. Experimentally, we form coincidence images in the near and far fields of a source of entangled photons and find that the product of their resolutions is a factor of 3 better than that which is possible according to classical diffraction theory.

Coincidence imaging can be understood in much the same way whether the source is entangled or classically correlated. In either case, one has a source which emits light into two different regions of space. The source is in principle stochastic (although it need not be) and may be characterized by a set of states, each of which is associated with a particular pair of emitted optical waves. One wave, the "object wave," illuminates the object and is collected either by a bucket detector (in the case of a transmittance object) or a pinhole detector (in the case of a diffraction object). The other wave, the "reference wave," illuminates an imaging system. *A sharp image appears in the joint intensity (photon coincidence rate) of the two detectors if, for each state of the source, the reference wave illuminates a single point on the imaging detector and the object detector sees the intensity of the corresponding point in the desired image.* In the case of a transmittance object, the object wave must converge to the corresponding point on the object. For a diffraction object, the object wave must expose the corresponding part of the diffraction pattern to the pinhole detector.

In [10] we argued that classically correlated light sources could be used to reproduce the behavior of all the variations of coincidence imaging yet proposed, including ghost diffraction [15] and ghost holography [16]. We demonstrated this idea for the case of a transmittance object, using two beams with classically correlated directions to probe and record the transmittance of the object point by point. Since point-by-point imaging is generally associated with incoherent imaging, it is less obvious that images formed by optical interference, such as diffraction patterns and holograms, can be formed using such a classical light source. To verify that these types of coincidence images can be formed without the benefit of entanglement, we have formed a ghost diffraction pattern of a double slit with two classically correlated beams (Fig. 1). The slits were 150 μm wide with centers separated by 450 μm. The light source consisted of a HeNe laser, a rotating mirror, a beam splitter, and a lens. The rotating mirror and the beam splitter produced two beams with varying, but correlated, directions of propagation. The mirror was mounted to a galvonometer
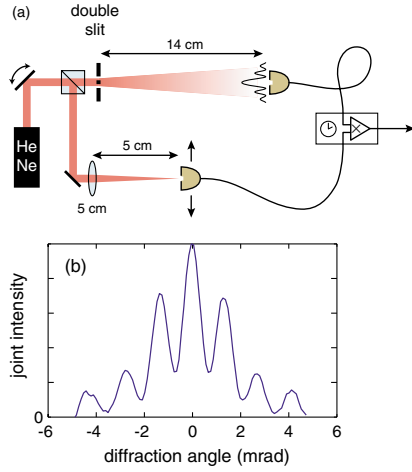
FIG. 1 (color online). (a) Setup used to perform coincidence diffraction with a classically correlated source. (b) The experimentally obtained diffraction pattern.

and was scanned repetitively at several Hz. The lens was used to focus one of the two beams onto a small-area (0.04 mm^2) detector mounted on a translation stage. The other beam illuminated the double slits, generating a diffraction pattern that was sampled by a second small-area detector. The signals from the two detectors were recorded on a digital oscilloscope. By measuring the average of the product of these two signals over a 10 s interval, we obtained the average value of the joint intensity. This measurement was repeated for different positions of the translation stage to obtain the results shown in Fig. 1.

The various types of coincidence imaging which have been proposed so far all involved a fixed geometry. In these cases one can associate each point in the image with a single state of the source. This fact is highly significant: if the intensity at each pixel is independent of any interference between states, then the same image can be formed using a source in a classical mixture of those states. As we show, a measurement of both photon position and transverse wave vector correlations can reveal the presence of quantum interference and distinguish a quantum light source from a classical one.

Consider a classical stochastic light source which emits a certain pair of waves in each state s. For each wave $j = 1, 2$, the width Δx in position and width Δk in transverse wave vector must satisfy the space-bandwidth uncertainty product [17]

$$\Delta x_{j,s}^2 \Delta k_{j,s}^2 \geq \tfrac{1}{4}. \tag{1}$$

More precisely, Δf_s^2 denotes the variance of the quantity f where the weighting function (or probability density) is the intensity of the wave, as a function of either position or transverse wave vector accordingly. Now, for a given state the joint intensity distribution is factorable and the variances in the quantities $x_- \equiv x_1 - x_2$ and $k_+ \equiv k_1 + k_2$ [18] are

$$\Delta x_{-,s}^2 = \Delta x_{1,s}^2 + \Delta x_{2,s}^2, \tag{2}$$

$$\Delta k_{+,s}^2 = \Delta k_{1,s}^2 + \Delta k_{2,s}^2, \tag{3}$$

with the result that $\Delta x_{-,s}^2 \Delta k_{+,s}^2 \geq 1$. Intuitively, one understands that if the source is in a classical mixture of states, then the joint uncertainty product for the entire ensemble cannot be smaller than that of any individual state. As a confirmation of this intuition, we note that the expected variance of f over the ensemble of states satisfies $\Delta f^2 \geq \sum_s P_s \Delta f_s^2$, so that

$$\Delta x_-^2 \Delta k_+^2 \geq \sum_{s,s'} P_s P_{s'} [\Delta x_{1,s}^2 \Delta k_{1,s'}^2 + \Delta x_{2,s}^2 \Delta k_{2,s'}^2$$
$$+ \Delta x_{1,s}^2 \Delta k_{2,s'}^2 + \Delta x_{2,s}^2 \Delta k_{1,s'}^2]. \tag{4}$$

With the use of Eq. (1) one obtains

$$\Delta x_-^2 \Delta k_+^2 \geq \frac{1}{8} \sum_{s,s'} P_s P_{s'} \left[\frac{\Delta x_{1,s}^2}{\Delta x_{1,s'}^2} + \frac{\Delta x_{2,s}^2}{\Delta x_{2,s'}^2} + \frac{\Delta x_{1,s}^2}{\Delta x_{2,s'}^2} + \frac{\Delta x_{2,s}^2}{\Delta x_{1,s'}^2} + \text{the same terms with } s \leftrightarrow s' \right] \tag{5}$$

$$\geq \frac{1}{8} \sum_{s,s'} P_s P_{s'} (2 + 2 + 2 + 2) = 1. \tag{6}$$

Thus, any source of classically correlated fields must obey the *joint uncertainty product*

$$\Delta x_- \Delta k_+ \geq 1. \tag{7}$$

Equation (7) is a fundamental relation arising from Fourier theory and is applicable to any pair of classical fields. Like a Bell inequality for continuous variables [19], it provides a statistical test for nonclassical behavior.

If the source is in a quantum superposition of states (i.e., an entangled state), the generalization from a single-state uncertainty product to an ensemble uncertainty product breaks down, and inequality (7) does not necessarily hold. For example, consider a quantum source in the ideal entangled state

$$|\psi\rangle = \int_{-\infty}^{\infty} |x, x\rangle dx. \tag{8}$$

The emitted photons are perfectly correlated in position. Through mathematical manipulation of Eq. (8), the source state $|\psi\rangle$ may also be written as

$$|\psi\rangle = \int_{-\infty}^{\infty} |k, -k\rangle dk, \tag{9}$$

where k denotes transverse wave vector. Thus a quantum source can produce a pair of fields which are perfectly correlated in position *and* perfectly (anti)correlated in transverse wave vector, whereas a classical source cannot. The quantum interference between states in one basis

allows for correlations to exist in the conjugate basis. As pointed out by Gatti *et al.* [11], the ability to form two coincidence images, one requiring near-field (position) correlations and one requiring far-field (transverse wave vector) correlations, should be a distinguishing feature of an entangled source. Based on the argument above, the signature of nonclassical behavior is a violation of Eq. (7).

To see whether the use of an entangled light source leads to a violation of Eq. (7), we illuminated a 2 mm-thick beta barium borate (BBO) crystal with 40 mW of 390 nm light (Fig. 2). This blue light was generated by frequency doubling the output of a 780 nm laser diode and was collimated at a diameter of ≈ 0.5 mm. By the process of parametric down-conversion, two fields of wavelength 780 nm were emitted nearly collinearly with the pump and with orthogonal polarizations. The generated fields were separated from the pump light by a prism and from each other by a polarizing beam splitter. The fields passed through 10 nm spectral filters and were then coupled by microscope objectives into two multimode fibers of core diameter 62 μm. The fibers were in turn coupled to two photon counting detectors and the count rates (both separately and in coincidence) were measured by NIM counter/timer modules. Approximately 3×10^6 pairs per second were generated in the modes measured by our imaging system. Because of filter losses, coupling losses, and detector inefficiencies, the maximum coincidence rate observed was 10% of the single-photon count rate in either arm. The coincidence time window was 6 ns.

An amplitude mask consisting of two opaque bars 200 μm wide and 200 μm apart was inserted into one arm. In this arm a high-power objective was used to demagnify the entire field of view onto the core of the fiber. In the other arm, a 5$\times$ objective was used with 1:1 magnification to couple a small portion of the field of view (one "pixel") into the fiber core. By scanning the fiber tip and recording the coincidence count rate, an image of the transmission profile of the mask was obtained. For near-field imaging, a 100 mm lens imaged the exit face of the BBO crystal onto the mask and onto the scanning fiber tip [Fig. 2(a)]. The geometry was such that the crystal was imaged with a magnification of 1.7. For far-field imaging, two lenses of focal length $f = 50$ mm were placed one focal length [20] away from the mask and the scanning fiber tip [Fig. 2(b)]. As expected, the entangled photons generated in the BBO crystal allowed well-resolved coincidence images to be formed in both the near and far fields. To determine the resolutions of the images, and thereby the joint uncertainty product, each image was compared to a simulated blurred image produced by convolving the ideal image with a Gaussian point spread function. The resolution of the image was taken to be the width of the point spread function which yielded the best agreement between the simulated and measured images. For the near-field case, the fit yielded a joint uncertainty $\Delta x_- = 33 \pm 14$ μm in the source plane. For the far-field case, the fit yielded a joint uncertainty in position of 65 ± 5 μm which corresponds to $\Delta k_+ = 11 \pm 1$ mm^{-1}. Thus the observed joint uncertainty product was $\Delta x_- \Delta k_+ = 0.35 \pm 0.15$, which is a clear violation of the classical inequality (7). That is, the product of the resolutions in the near and far fields was a factor of 3 better than is possible according to classical diffraction theory.

For the sake of comparison, a similar experiment was performed with light in a classical ensemble of states. In this experiment, the BBO was replaced by the correlated HeNe source described previously. For this experiment, the geometry was chosen so that at a designated "source plane" (indicated by a dashed line in Fig. 3) both the position and direction of the beam varied with the rotation of the mirror. The rotation range (≈ 20 mrad) and the beam size at the source plane (~ 50 μm) were chosen to yield nominally similar ranges (≈ 1 mm) and resolutions (~ 70 μm) at the object for both near- and far-field imaging geometries. Again, ensemble measurements were obtained by driving the mirror with an electric signal and averaging the results over a time long compared with the period of the signal. For this experiment, fibers and photon counting modules were not used. Instead, the intensity was measured by two silicon photodiodes with large (1 cm^2) and small (0.04 mm^2) active areas for the bucket and point detectors, respectively. The limit imposed by classical diffraction on the simultaneous correlation of position and direction is apparent: when the mask is well resolved in the far field [Fig. 3(b)], it is barely resolved in the near field [Fig. 3(a)]. Indeed, for these
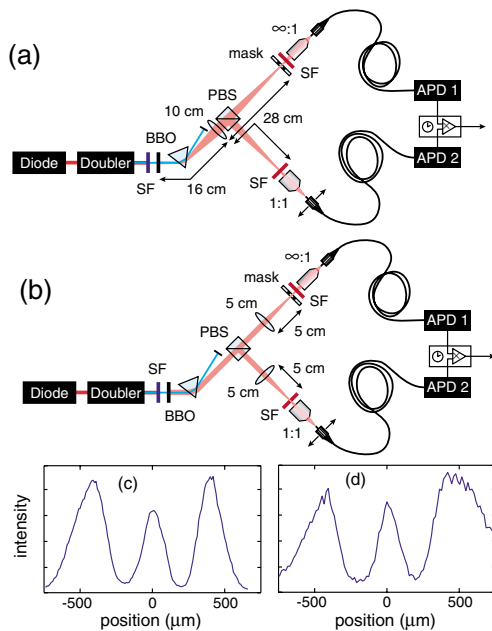

FIG. 2 (color online). Experimental setups used to form coincidence images of a 2-bar mask in the near field (a),(c) and far field (b),(d) of an entangled light source. PBS: polarizing beam splitter; SF: spectral filter.
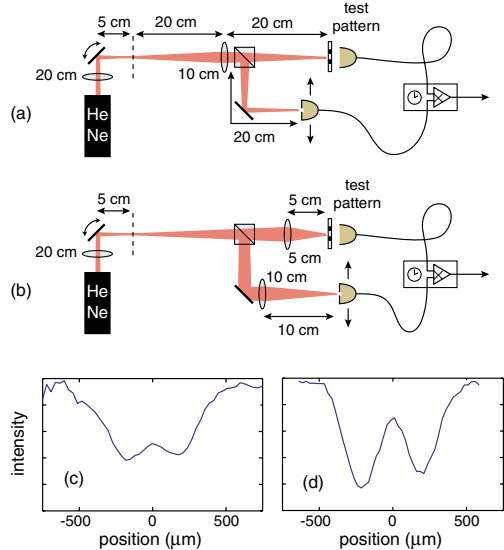
FIG. 3 (color online). Experimental setups used to form coincidence images of a 2-bar mask in the near field (a),(c) and far field (b),(d) of a classically correlated light source.

images we obtain $\Delta x_- \Delta k_+ = 1.5$ in agreement with Eq. (7).

As a final point, we note that the state described by Eqs. (8) and (9) may be written as an entangled superposition of states in *any* basis of field modes. Therefore an ideal entangled light source possesses strong correlations in whichever basis addresses the pixels of the chosen image plane. Consequently, a fixed source of entangled light allows for high-resolution coincidence imaging in any plane. As evidenced by Eq. (7), classically correlated light sources are limited in this respect. Interestingly, a recent calculation by Gatti *et al.* [21] reveals that the *fluctuations* of a classically correlated field are not constrained by Eq. (7) and may be used to form sharp images, albeit with a background, in both near and far fields.

In summary, we have argued that one can understand image formation in coincidence imaging methods as a point-by-point process, in which each pixel is addressed by a different state of the source. Since interference between states is not required to form the image, one knows that the image may also be formed using a light source in a classical mixture of those states. We confirmed this idea by forming a coincidence image of the diffraction pattern of a double slit using a classically correlated light source. Furthermore, we have argued that strong correlations between pairs of conjugate variables are a signature of nonclassical behavior, and we have derived a continuous-variable inequality which quantifies this idea. In the context of coincidence imaging, the nonclassical signature is the ability to form sharp, high-contrast images in multiple planes with a fixed source. With the use of entangled photons, we formed two images whose resolutions had a product that was 3 times better than is possible according to classical diffraction theory, thereby demonstrating distinctly nonclassical behavior in a coincidence imaging experiment.

*Electronic address: bennink@optics.rochester.edu
†Present address: Department of Physics, Adelphi University, Garden City, NY 11530, USA.

[1] C. Bennett, F. Bessette, G. Brassard, L. Salvail, and J. Smolin, J. Cryptology **5**, 3 (1992).

[2] D. Bouwmeester, K. Mattle, J. Pan, H. Weinfurter, A. Zeilinger, and M. Zukowski, Appl. Phys. B **67**, 749 (1998).

[3] K. Mattle, H. Weinfurter, P. Kwiat, and A. Zeilinger, Phys. Rev. Lett. **76**, 4656 (1996).

[4] A. Malygin, A. Penin, and A. Sergienko, Pis'ma Zh. Eksp. Teor. Fiz. **33**, 493 (1981) [JETP Lett. 33, 477 (1981)].

[5] A. F. Abouraddy, K. C. Toussaint, Jr., A. V. Sergienko, B. E. A. Saleh, and M. C. Teich, Opt. Lett. **26**, 1717 (2001).

[6] A. N. Boto, P. Kok, D. S. Abrams, S. L. Braunstein, C. P. Williams, and J. P. Dowling, Phys. Rev. Lett. **85**, 2733 (2000).

[7] M. D'Angelo, M. Chekhova, and Y. Shih, Phys. Rev. Lett. **87**, 013602 (2001).

[8] E. Nagasako, S. Bentley, R. Boyd, and G. Agarwal, Phys. Rev. A **64**, 43802 (2001).

[9] T. B. Pittman, Y. H. Shih, D. V. Strekalov, and A. V. Sergienko, Phys. Rev. A **52**, R3429 (1995).

[10] R. Bennink, S. Bentley, and R. Boyd, Phys. Rev. Lett. **89**, 113601 (2002).

[11] A. Gatti, E. Brambilla, and L. Lugiato, Phys. Rev. Lett. **90**, 133603 (2003).

[12] M. D'Angelo and Y. Shih, quant-ph/0302146.

[13] M. Rubin, quant-ph/0303188.

[14] J. S. Bell, Physics (Long Island City, N.Y.) **1**, 195 (1965).

[15] D. V. Strekalov, A. V. Sergienko, D. N. Klyshko, and Y. H. Shih, Phys. Rev. Lett. **74**, 3600 (1995).

[16] A. F. Abouraddy, B. E. A. Saleh, A. V. Sergienko, and M. C. Teich, Opt. Express **9**, 498 (2001).

[17] W. C. Elmore and M. A. Heald, *Physics of Waves* (Dover Publications, Inc., New York, 1985).

[18] We consider these particular quantities because entangled photons generated by parametric down-conversion are typically correlated in position and anticorrelated in wave vector.

[19] Z. Ou, S. Pereira, H. Kimble, and K. Peng, Phys. Rev. Lett. **68**, 3663 (1992).

[20] The field in the back focal plane of a lens is the Fourier transform of the incident field, with the coordinate x in this plane corresponding to the wave number $(2\pi/\lambda f)x$.

[21] A. Gatti, E. Brambilla, M. Bache, and L. Lugiato, quant-ph/0307187.